

Enhancement of G Protein–Coupled Signaling by DHA Phospholipids

Drake C. Mitchell, Shui-Lin Niu, and Burton J. Litman*

Laboratory of Membrane Biochemistry and Biophysics, National Institute on Alcohol Abuse and Alcoholism, Bethesda, Maryland 20892–8115

ABSTRACT: The effect of phospholipid acyl chain and cholesterol composition on G protein–coupled signaling was studied in native rod outer segment (ROS) disk and reconstituted membranes by measuring several steps in the visual transduction pathway. The cholesterol content of disk membranes was varied from 4 to 38 mol% cholesterol with methyl- β -cyclodextrin. The visual signal transduction system [rhodopsin, G protein (G_t), and phosphodiesterase (PDE)] was reconstituted with membranes containing various levels of phospholipid acyl chain unsaturation, with and without cholesterol. ROS membranes from rats raised on n-3 fatty acid–deficient and –adequate diets were also studied. The ability of rhodopsin to form the active metarhodopsin II conformation and bind G_t was diminished by a reduction in the level of DHA (22:6n-3) acyl chains or an increase in membrane cholesterol. DHA acyl chain containing phospholipids minimized the inhibitory effects of cholesterol on the rate of rhodopsin- G_t coupling. The activity of PDE, which is a measure of the integrated signal response, was reduced in membranes lacking or deficient in DHA acyl chains. PDE activity in membranes containing docosapentaenoic acid (DPA, 22:5n-6) acyl chains, which replace DHA in n-3 fatty acid deficiency, was 50% lower than in DHA-containing membranes. Our results indicate that efficient and rapid propagation of G protein–coupled signaling is optimized by DHA phospholipid acyl chains.

Paper no. L9196 in *Lipids* 38, 437–443 (April 2003).

Many of the functions associated with biological membranes, e.g., signal transduction, ion movement, or energy conversion, are carried out by membrane proteins. A wide range of diseases, psychiatric disorders, and dietary conditions are likely due to changes in membrane phospholipid composition and cholesterol content (see Refs. 1 and 2 for recent reviews), which in turn lead to altered protein function and subsequent

illness. Most biological membranes undergo constant remodeling and renewal, and their lipid composition is readily altered by changes in the lipid precursor components made available by diet and metabolism. Thus, diet and disease can readily alter the lipid composition of membranes, although, in general, only genetic mutations alter protein function directly. To understand how the function of biological membranes is impaired or altered by changes in membrane lipid composition, it is necessary to understand how membrane lipids and proteins interact with each other and among themselves, so as to carry out a wide range of biological functions.

One of the principal compositional variables of biological membranes subject to dietary influence is the content of highly polyunsaturated phospholipid acyl chains. A large body of research demonstrates the need for high levels of polyunsaturated fats, particularly n-3 polyunsaturates, for optimal infant development and performance in later life (3–5). The conclusions drawn from decades of research on nutrition strongly suggest that specific, but unidentified, biochemical processes are optimized by the presence of n-3 polyunsaturates and/or compromised by their absence. The phospholipids of neuronal and retinal cells are rich in highly unsaturated acyl chains, especially those of DHA. Much previous work demonstrated that DHA-containing phospholipids enhance the formation of the active metarhodopsin II (MII) conformation of photoactivated rhodopsin (6–8). In this report, we demonstrate that multiple aspects of G protein–coupled signal transduction require DHA phospholipid acyl chains for optimal functional efficacy and that this requirement for DHA phospholipid acyl chains is related to the unique acyl chain packing properties imparted by DHA.

The G protein–coupled motif is a fundamental and widespread mode of intracellular signaling; it includes the sensory pathways for vision, olfaction, taste, touch, and a variety of neurotransmitters, including dopamine, serotonin, γ -amino butyric acid (GABA), and histamine (9). Each of these chemical and physical agents acts upon a unique integral membrane receptor protein, which is embedded in a lipid membrane. Many of the membranes that contain significant amounts of G protein–coupled signaling activity, such as neuronal and retinal tissues and the olfactory bulb, contain high levels of the n-3 polyunsaturated acyl chain derived from DHA (10,11). Dietary n-3 fatty acid deficiency leads to the replacement of DHA phospholipid acyl

*To whom correspondence should be addressed at Park Bldg., Room 158, MSC 8115, 12420 Parklawn Dr., Bethesda, MD 20892–8115.
E-mail: litman@helix.nih.gov

Abbreviations: DPA, docosapentaenoic acid, 22:5n-6; DPH, 1,6-diphenyl-1,3,5-hexatriene; DTPA, diethylenetriamine pentaacetic acid; ERG, electroretinogram; f_v , membrane free volume parameter; GABA, γ -amino butyric acid; G_t , transducin; K_a , MII- G_t association constant; K_{eq} , MI-MII equilibrium constant, [MII]/[MI]; MBCD, methyl- β -cyclodextrin; MI, metarhodopsin I; MII, metarhodopsin II; PDE, phosphodiesterase; Rh*, fraction of rhodopsin molecules that absorb a photon; ROS, rod outer segment; TBS, Tris basal salt.

chains with docosapentaenoic acid (DPA) acyl chains in these membranes (12). The functional significance of DHA is demonstrated by impaired visual response (13,14), learning deficits (11,15), loss of odor discrimination (16), and reduced spatial learning (17) associated with n-3 fatty acid deficiency. These findings suggest that a high level of DHA in membrane phospholipids is required for optimal function of a number of diverse signaling pathways. A common feature of these pathways is the central role of G protein-coupled signaling.

Receptors in the G protein-coupled superfamily are integral membrane proteins, consisting of seven transmembrane helices and their respective connecting loops. The ligand-binding site on the receptor is formed by transmembrane helices and generally lies near the midpoint of the membrane; hence, the conformational changes accompanying receptor activation would be expected to have a dependence on the physical properties of the membrane lipid bilayer. The G protein and effector proteins are generally peripheral proteins, bound to the membrane by a combination of an isoprenoid chain-lipid bilayer interaction (18,19) and electrostatic forces (20). The interaction of the G protein with the receptor occurs in the hydrophilic region of the protein, external to the membrane bilayer (21,22). In this study, we asked whether the composition and physical properties of the hydrophobic core of the membrane might affect the interaction between the receptor and the G protein that occurs external to the membrane bilayer.

After absorption of light by 11-*cis* retinal, rhodopsin exists as an equilibrium mixture of an active conformation, MII, and an inactive conformation, metarhodopsin I (MI) (see Ref. 23 for a review). Each MII activates several hundred transducin (G_t) molecules, which then activate the effector enzyme, a cGMP-specific phosphodiesterase (PDE). The activated PDE catalyzes the hydrolysis of cGMP, triggering closure of cGMP-gated $\text{Na}^+/\text{Ca}^{2+}$ channels in the plasma membrane, leading to hyperpolarization of the rod outer segment (ROS) and the visual response. In this study, we reconstituted rhodopsin, G_t , and PDE into large, unilamellar vesicles containing varied levels of unsaturated acyl chains and cholesterol. In addition, we purified ROS disk membranes from rats raised on either an n-3 fatty acid-deficient or -adequate diet. Our results demonstrate that the degree of unsaturation in the acyl chain and the level of cholesterol in the membrane significantly affect MII formation, MII· G_t coupling efficiency and speed, and PDE activity. Because the visual signaling system is the prototype member in the superfamily of G protein-coupled signaling systems, our findings regarding the effect of lipid composition and cholesterol on receptor-G protein coupling may well serve as a general demonstration of the modulation of cell signaling by changes in membrane composition.

EXPERIMENTAL PROCEDURES

Sample preparation. Cholesterol and methyl- β -cyclodextrin (MBCD) were purchased from Sigma Chemical (St. Louis, MO). The cholesterol-MBCD complex was prepared by pre-

mixing cholesterol and MBCD as solids (weight ratio of 1:20) followed by solubilization in degassed Tris basic salt (TBS) buffer consisting of 10 mM Tris, 60 mM NaCl, 30 mM KCl, and 50 μM diethylenetriamine pentaacetic acid (DTPA), pH 7.5. The solution was sealed in argon and shaken at room temperature overnight. The final solution was filtered through a 0.45- μm filter and assayed for final cholesterol concentration. The cholesterol CII assay kit was from Wako (Wako Chemicals, Richmond, VA). The bicinchoninic acid and Coomassie Plus protein assay kits were from Pierce (Pierce Chemical, Rockford, IL). Bovine ROS were isolated from frozen retinas (James and Wanda Lawson, Lincoln, NE) (24) and intact rod disk membranes were isolated from ROS by centrifugation on a ficol gradient (25). For reconstitution in vesicles with defined lipid composition, rhodopsin was solubilized in octylglucoside and purified on a concanavalin A affinity column (26). Phospholipids were purchased from Avanti Polar Lipids (Alabaster, AL) and their purity was ascertained by HPLC. Large unilamellar vesicles containing rhodopsin at a ratio of 1 rhodopsin to 100 phospholipids were prepared using the rapid dilution technique (27). After dialysis to remove detergent, all vesicle preparations were suspended in pH 7.5 Tris basal salt (TBS) buffer consisting of 10 mM Tris, 60 mM NaCl, 30 mM KCl, and 50 mM DTPA. G_t was prepared from ROS as a hypotonic extract (28) and stored in pH 7.5 TBS buffer with 30% glycerol at -20°C for no longer than 2 wk. All preparation of phospholipids was carried out in an argon-filled glove box and in thoroughly degassed buffers due to the susceptibility to oxidation of polyunsaturated phospholipids. The phospholipid, cholesterol, and rhodopsin content of each reconstituted vesicle preparation was determined by independent phosphate (29), cholesterol, and rhodopsin (27) assays, respectively.

Samples for equilibrium absorbance measurements and PDE activity measurements were suspended in TBS buffer at 7.5 μM rhodopsin. Samples for fluorescence measurements were made immediately before use by diluting a concentrated vesicle or ROS disk membrane stock solution to 150 μM phospholipid, and adding 0.5 μL of 1,6-diphenyl-1,3,5-hexatriene (DPH) in tetrahydrofuran to yield a final phospholipid to DPH ratio of 300:1.

Cholesterol-depleted disk membranes were prepared by incubating disk membranes with 10 mM MBCD in TBS buffer, pH 7.5. Samples were incubated at room temperature in the dark for 2 h on a shaker. Measurements of disk cholesterol content at several time points indicated that 2 h was a sufficient incubation time to reach equilibrium for cholesterol exchange between disk membranes and MBCD (30). The MBCD-treated disk membranes were then separated from MBCD by centrifugation followed by two additional washes in TBS buffer. The membrane pellet and MBCD-containing supernatant were assayed for cholesterol, phospholipids (29), and rhodopsin (27), and the mole fraction of cholesterol to total phospholipids in disk membranes was determined. Cholesterol-enriched disk membranes were prepared similarly, except that disk membranes were incubated with cholesterol-

loaded MBCD (0–1.2 mM cholesterol in 10 mM MBCD). The following mol% samples were used in this study: 4, 12, 15, and 38 mol%. The 15 mol% cholesterol sample comprised native disk membranes without MBCD treatment.

Measurements. The MI-MII equilibrium in the absence and presence of G_t was measured in isotonic buffer at pH 7.5 using a series of equilibrium absorption spectra, as previously described (31). The amount of additional MII formed in the presence of G_t is proportional to the amount of MII· G_t complex formed; thus, MII· G_t binding constants were determined from a series of measurements with varying ratios of rhodopsin to G_t . The kinetics of both MII and MII· G_t formation were assessed by measuring the transient absorption at 380 nm using a flash photolysis system constructed in the laboratory. The kinetic data were analyzed in terms of a microscopic photoreaction model, as described previously (32).

PDE activity was assayed using a continuous pH method (33) with minor modifications. Samples were preincubated with the pH electrode in a thermoregulated 1-mL quartz cuvette and bleached by a light pulse that was attenuated with neutral density filters to obtain the desired bleaching level of rhodopsin. The bleaching flash was triggered after acquisition of a preflash baseline.

Fluorescence lifetime and differential polarization measurements were performed with a K2 multifrequency cross-correlation phase fluorometer (ISS, Urbana, IL) as previously described (34). For lifetime measurements, 12 modulation frequencies were used, logarithmically spaced from 5 to 200 MHz, and differential polarization measurements were made at 15 modulation frequencies logarithmically spaced from 5 to 200 MHz. Both total intensity decay and differential polarization measurements were repeated with each membrane composition a minimum of three times. Measured polarization-dependent differential phases and modulation ratios for each sample were combined with the measured total intensity decay to yield the anisotropy decay, $r(t)$. Anisotropy decays of DPH were analyzed using the Brownian rotational diffusion model (35). This model characterizes the anisotropy decay of DPH in terms of the orientational distribution function, $f(\theta)$, and the diffusion coefficient for rotation about the long axis of DPH. The orientational distribution function was used to derive the membrane free volume parameter, f_v , which is proportional to the overlap of $f(\theta)$ with a random orientational distribution (35,36).

Analysis. All data analysis was performed with NONLIN (37) with subroutines specifying the particular functions required for the different types of measurements written by the authors. NONLIN uses the Gauss–Newton method to perform nonlinear least-squares analysis while accounting for the SD of the measurement associated with each independent data point. Measurement SD was obtained from the noise in the preflash signal, in the case of the kinetic absorption and PDE activity measurements, or from the statistical analysis performed by the acquisition software in the case of the equilibrium absorption measurements and all fluorescence measurements. NONLIN returns the optimized parameter values as

well as asymmetric confidence intervals corresponding to 1 SD. The asymmetry of all parameter values was <15%; thus, the high and low SD were averaged to obtain the reported values of 1 SD. All measurements were repeated 3–6 times and each trial was analyzed independently. The results of separate trials were averaged by weighting the results of each trial with its associated SD. Statistical significance was assessed from *P*-values resulting from Student's *t*-test with two-tailed distributions and two-sample unequal variance.

RESULTS

The effect of membrane cholesterol on both rhodopsin activation and acyl chain packing was investigated in ROS disk membranes by using MBCD to vary the membrane cholesterol content (30). An inverse correlation between the membrane cholesterol content and the MI-MII equilibrium constant (K_{eq}) was observed at 37°C. In control disk membranes, the cholesterol concentration was 15 mol% and K_{eq} was 0.81 ± 0.08 at 37°C. In disk membranes depleted of cholesterol to a level of 4 mol%, K_{eq} was 1.00 ± 0.10 , whereas in membranes enriched to 38 mol% cholesterol, K_{eq} was reduced to 0.73 ± 0.11 . Variation in the cholesterol content of disk membranes also resulted in substantial changes in the motional and orientational properties of the hydrophobic fluorescence probe DPH. A series of studies demonstrated that the overall orientational order of DPH in a phospholipid bilayer is well summarized by the parameter f_v , a measure of phospholipid acyl chain packing free volume (35,38). At 37°C, reduction of membrane cholesterol to 4 mol% increased f_v by 45% relative to control disks, whereas enrichment of cholesterol to 38 mol% reduced f_v by 30% relative to control disks. The values of K_{eq} and f_v at 37°C produced by variation in membrane cholesterol are linearly related, as shown in Figure 1. Previous measurements show that K_{eq} and f_v are linearly related with respect to changes in temperature and membrane cholesterol content (39,40) for rhodopsin reconstituted with a number of specific PC. The data summarized in Figure 1 demonstrate that the positive correlation between bilayer free volume and the formation of MII is a general property of the MII conformation that is manifest in natural as well as synthetic membranes.

The effects of DHA phospholipid acyl chains and cholesterol on the early steps in G protein-coupled signaling were addressed in a series of experiments utilizing purified rhodopsin reconstituted into vesicles consisting of di22:6PC, 18:0,22:6PC, and 18:0,18:1PC with and without cholesterol (41). In the absence of G_t , K_{eq} followed the order di22:6PC > 18:0,22:6PC > 18:0,22:6PC + 30 mol% cholesterol > 18:0,18:1PC > 18:0,18:1PC + 30 mol% cholesterol. This is consistent with previous findings (8,40) that reduced acyl chain polyunsaturation and the presence of cholesterol reduced the amount of MII formation. Membrane lipid composition and cholesterol also modulate the binding of MII to G_t (41). Increasing acyl chain unsaturation from 18:0,18:1PC to 18:0,22:6PC resulted in a threefold enhancement in the MII· G_t

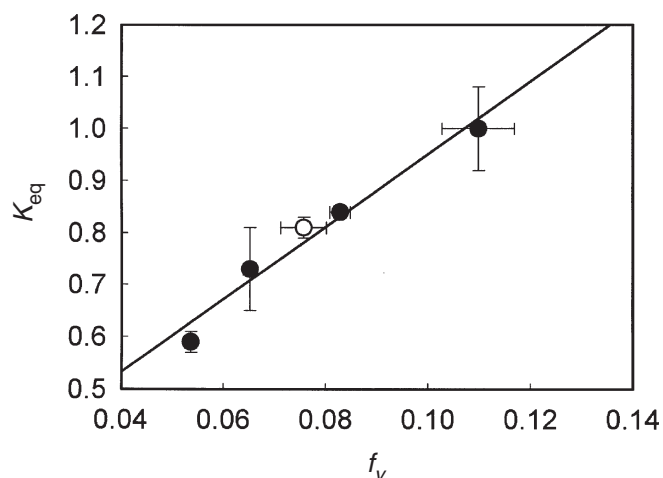


FIG. 1. Linear correlation of the metarhodopsin I (MI)-metarhodopsin II (MII) equilibrium constant, K_{eq} , and the phospholipid acyl chain packing free volume parameter, f_v , from bovine rod outer segment (ROS) disk samples with varying cholesterol concentrations at 37°C. The unfilled circle is the control disk at 15 mol% cholesterol, which received no methyl- β -cyclodextrin (MBCD) treatment. From left to right, the membrane cholesterol concentrations are 38, 30, 15, 12, and 4 mol% (see Fig. 6 in Ref. 30).

association constant, K_a . Further increase in unsaturation to di22:6PC resulted in a reduction in K_a relative to 18:0, 22:6PC. Cholesterol reduced K_a in both monounsaturated 18:0,18:1PC and polyunsaturated 18:0,22:6PC.

Combining the effects of membrane composition on receptor activation and receptor-G protein binding affinity reveals the net effect of membrane composition on the overall efficiency of formation of the receptor-G protein complex. Efficiency in this context refers to the fraction of rhodopsin molecules that absorb a photon, designated Rh^* , and succeed in binding G_t . Thus, efficiency is denoted by the ratio $[MII \cdot G_t]/[Rh^*]$. In the rod cell, the ratio of rhodopsin to G_t is ~10:1 and only ~1 rhodopsin/100,000 absorbs a photon and is activated (see Ref. 42 for a review), with each rhodopsin activating several hundred G_t molecules to produce a visual response. Thus, the differences in the efficiency of receptor-G protein complex formation shown in Figure 2 are significant. Approximately 90% of the rhodopsin molecules that absorb a photon form a complex with G_t in 18:0, 22:6PC and di22:6PC vesicles, but only 60% succeed in binding G_t in 18:0,18:1PC vesicles. The presence of 30 mol% cholesterol resulted in only ~60 and 30% of photoactivated rhodopsin molecules forming a complex with G_t in 18:0,22:6PC and 18:0,18:1PC, respectively.

The time course of the formation of both MII and the MII·G complex after an activating flash was measured at physiologic temperature for rhodopsin in membranes consisting of 18:0,22:6PC, and 18:0,18:1PC with and without 30 mol% cholesterol (32). Complete analysis of the kinetic data acquired at 37°C showed that the time constants for MII, $\tau(MII)$, were in the order 18:0,22:6PC < 18:0,22:6PC/30 mol% cholesterol < 18:0,18:1PC < 18:0,18:1/30 mol% cholesterol, with values of 0.55 ± 0.06 , 0.68 ± 0.07 , 1.13 ± 0.1 , and 1.83 ± 0.11 ms, respectively. Uncertainties are given as 1 SD, and all values of

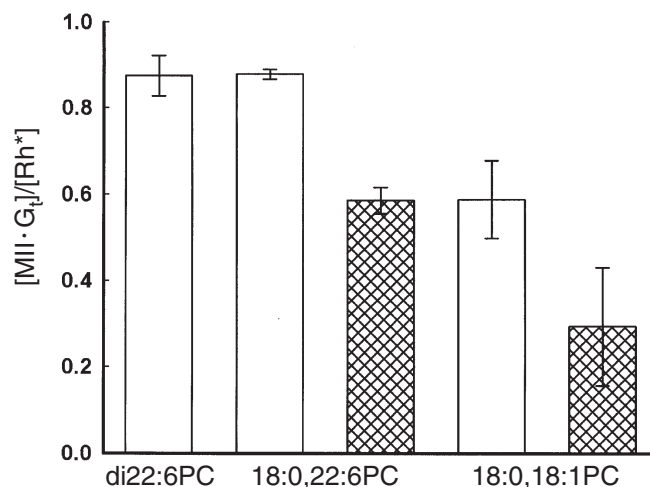


FIG. 2. Effect of 22:6 acyl chains and cholesterol on the efficiency of receptor-G protein coupling. The ratio $[MII \cdot G_t]/[Rh^*]$ is the fraction of photoactivated rhodopsin that binds transducin (G_t) and thereby participates in signal transduction. Cross-hatched bars correspond to bilayers that include 30 mol% cholesterol. Value for 18:0,18:1PC/30 mol% cholesterol is significantly different from all others with $P < 0.01$, and values for both 18:0,22:6PC/30 mol% cholesterol and 18:0,18:1PC are significantly different from both di22:6PC and 18:0,22:6PC, $P < 0.005$ (see Fig. 5 in Ref. 41). Rh^* , fraction of rhodopsin molecules that absorb a photon; for other abbreviation see Figure 1.

$\tau(MII)$ were significantly different from each other, $P < 0.03$. The time constant for MII· G_t complex formation, $\tau(MII \cdot G_t)$, varied in the same order as $\tau(MII)$. The ratio $\tau(MII \cdot G_t)/\tau(MII)$ is an informative quantity with respect to understanding how membrane composition may alter the diffusion-dependent aspects of G protein-coupled signaling. Values of this ratio slightly >1 indicate that the receptor-G protein complex is formed nearly as rapidly as possible, whereas values significantly >1 indicate that the activated receptor must wait a period of time for a fruitful collision with G protein. Cholesterol has very little effect on the diffusion-dependent kinetics of MII· G_t formation in a 18:0,22:6PC bilayer (Fig. 3). This is consistent with a number of measurements that show that cholesterol has its smallest effect on the properties of bilayers containing DHA acyl chains (43). In contrast, in an 18:0,18:1PC bilayer, cholesterol increases the time required for MII formation by 50%, and quadruples the time required for MII· G_t formation, resulting in a value of $\tau(MII \cdot G_t)/\tau(MII)$ of nearly 3. In 18:0,22:6PC at 37°C, MII formation occurs in 0.55 ms, and MII and MII· G_t complex formation are nearly coincident. Because MII cannot react with G_t any more quickly than it is formed from MI, the rate of formation of the MII· G_t complex in 18:0,22:6PC appears to be maximal. In 18:0,22:6PC, the rate of MII· G_t complex formation, which is limited by lateral diffusion, is altered only slightly by the presence of 30 mol% cholesterol, further suggesting that 18:0,22:6PC has the optimal acyl chain composition for rapid formation of receptor-G protein complex among the PC examined in this study.

It is informative to assess directly the integrated response of the G protein-coupled signaling pathway by measuring the

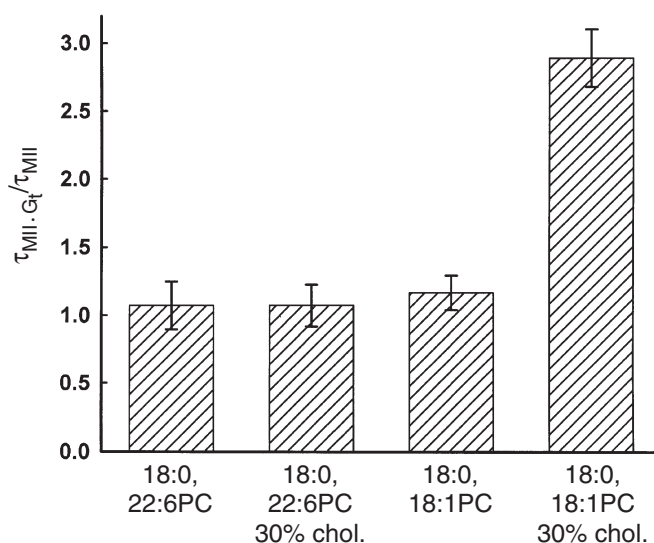


FIG. 3. Summary of the effects of phospholipid acyl chain composition and bilayer cholesterol content on the ratio of the time constants for MII and MII · G_t complex formation at 37°C. The processes that lead to formation of both the MII conformational state and the MII · G_t complex consist of multiple kinetic steps (32). The average time constants were used in the formulation presented here to facilitate comparison between the different membrane compositions of the overall time course of signal transduction. The value for 18:0,18:1/30 mol% cholesterol is significantly different from the other three values, $P < 0.001$ (recalculated from data in Fig. 5 of Ref. 32). For abbreviations see Figures 1 and 2.

activity of the PDE. In visual signal transduction, PDE activity is highly amplified relative to the initial stimulus and would be expected to be sensitive to any alteration in functional efficiency of the receptor and/or G protein. For this reason, we examined PDE activity in large unilamellar vesicles containing rhodopsin, G_t, and PDE reconstituted in three different PC with small but significant variations in the composition of the polyunsaturated *sn*-2 acyl chain. The three PC all had an 18:0 acyl chain at the *sn*-1 position and DHA, DPA, or 22:5n-3 acyl chains at the *sn*-2 position. At a light stimulus level of 1 bleached rhodopsin/20,000 rhodopsins, the PDE activity in the two n-3-containing membranes was twice as high as in the DPA membrane, as shown in Figure 4.

DISCUSSION

The results presented here demonstrate that membrane lipid composition modulates several steps in G protein-coupled signal transduction. Increased membrane cholesterol and phospholipid acyl chain saturation both have inhibitory effects on this important form of signal transduction. These two compositional variables appear to modulate membrane protein function *via* the same physical mechanism, that is, by increasing phospholipid acyl chain packing order. Cholesterol-induced changes in the level of activated rhodopsin, MII, as measured by K_{eq} , and acyl chain packing, as measured by f_v , are linearly related over the entire range of cholesterol concentrations examined (Fig. 1). A linear correlation between changes in K_{eq} and f_v induced by changes in bilayer chole-

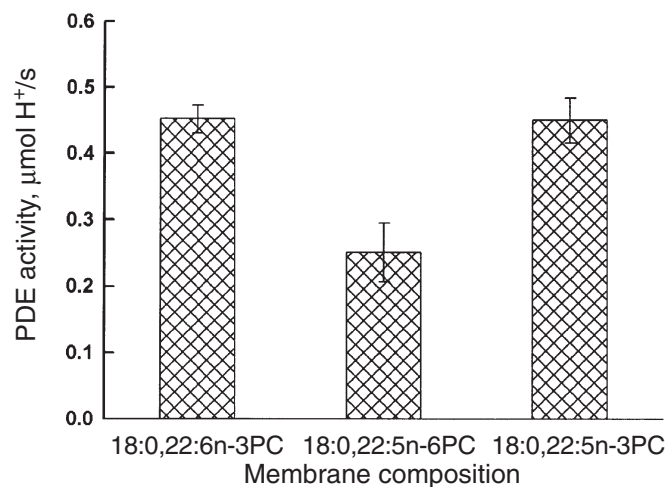


FIG. 4. Comparison of activities of the effector enzyme, phosphodiesterase (PDE), for rhodopsin, G_t, and PDE reconstituted in three membranes containing PC with a 22-carbon, polyunsaturated *sn*-2 acyl chain. The light intensity for this comparison was sufficient to bleach one rhodopsin per 20,000 rhodopsins, which is within the range of stimulus conditions associated with normal rod cell vision. 18:0,22:6n-3PC and 18:0,22:5n-3PC did not differ, but 18:0,22:5n-6 was significantly different from both of them, $P < 0.005$. For other abbreviation see Figure 2.

sterol was observed previously in studies of rhodopsin reconstituted in phospholipid membranes (39,40). In addition, temperature-induced changes in K_{eq} and f_v are linearly related for rhodopsin in ROS disk membranes and in reconstituted phospholipid vesicles (40,44). It is significant that the correlation shown in Figure 1 was obtained for measurements at 37°C, demonstrating that cholesterol causes correlated changes in acyl chain packing and rhodopsin activation at physiologic temperature. The MI to MII transition is accompanied by a 100 mL/mol volume expansion (45); thus, a reduction of membrane free volume would impose an energy barrier that would reduce the equilibrium concentration of MII. K_{eq} and f_v are linearly correlated over the entire range of membrane cholesterol concentration examined, and cholesterol had no observable structural perturbation on rhodopsin, leading us to conclude that cholesterol inhibits rhodopsin activation *via* an indirect effect of cholesterol on phospholipid acyl chain packing, i.e., by a free volume-mediated mechanism.

Previous studies showed that both decreased phospholipid acyl chain unsaturation and increased cholesterol concentration reduce the formation of MII *via* a mechanism linked to the specific packing properties of polyunsaturated acyl chains, DHA in particular, and the effect of cholesterol on these packing properties (40,41,44). The results presented here demonstrate that the functional ramifications of DHA acyl chains extend beyond the unimolecular transition from MI to MII to the rapid and efficient coupling of receptor and G protein, as well as the functional efficacy of the integrated signaling pathway as shown by the PDE effector enzyme activity. Current evidence indicates that G_t interacts with the three hydrophilic loops on the surface of rhodopsin, which means that the protein-protein interaction surfaces are external to the bilayer (46). The sensitivity of the MII · G_t binding

interaction to membrane composition (Figs. 2 and 3) demonstrates that protein–protein interactions, which occur on the hydrophilic surfaces of membrane proteins, are also affected by changes in membrane composition in the hydrophobic core of the membrane. This finding suggests for the first time that the protein–protein interactions, which occur on the hydrophilic surface of proteins, external to the membrane phospholipid bilayer, and are required in many signaling pathways, may be modulated by changes in the composition of the lipid hydrophobic core of the membrane.

The alterations in receptor conformation change, receptor-G protein binding strength and rate of receptor-G protein complex formation summarized in Figures 1–3 likely underlie the changes in PDE activity shown in Figure 4. This might reasonably be expected because the events measured in Figures 1–3 precede PDE activation in the G protein–mediated signaling cascade. The dependence of PDE activity on the presence of a polyunsaturated n-3 acyl chain at the *sn*-2 position (Fig. 4) clearly demonstrates that G protein–coupled signaling is exquisitely sensitive to phospholipid acyl chain unsaturation and double bond position. The reduced activity of PDE in 18:0,22:5n-6 PC compared with 18:0,22:6n-3 PC is a quantitative measure of the functional inequivalence of these two polyunsaturated phospholipid acyl chains. This comparison is crucial to our understanding of the biochemical basis for the effects of dietary n-3 fatty acid deficiency because such deficiency generally leads to the replacement of DHA with DPA (3).

To determine the effects of changes in membrane composition resulting from *in vivo* processes, we examined MII formation and PDE activity in ROS disk membranes purified from Long-Evans rats fed diets that were either adequate or deficient in n-3 fatty acids (Niu, S.-L., Mitchell, D.C., Lim, S.-Y., Wen, Z.-M., Kim, H.-Y., Salem, N., Jr., and Litman, B.J., unpublished data). The MI-III equilibrium constant was ~15% higher in the membranes from the n-3 fatty acid–adequate rats, but the difference was not significant. However, the membranes from the adequate rats produced a level of PDE activity that was nearly fivefold higher than in membranes from the n-3 fatty acid–deficient rats, and the difference was significant ($P < 0.001$, paired *t*-test). A detailed analysis of the phospholipid species present in these two ROS disk membranes is underway, but a preliminary fatty acid analysis shows that ~80% of the DHA in the ROS disk membranes of the n-3 fatty acid–adequate rats was replaced with DPA in the n-3 fatty acid–deficient rats. The changes in MII formation and PDE activity in ROS obtained from rats raised on n-3 fatty acid–adequate or –deficient diets are essentially identical to the results obtained with reconstituted vesicle systems and isolated bovine ROS disk membranes. Together, these results form a body of information that provides an understanding at the molecular level of the changes in electroretinogram (ERG) associated with dietary n-3 fatty acid deficiency in animals and nonhuman primates.

The results presented here suggest that the delays and reduced amplitude in ERG responses observed in dietary n-3 deficiency (14,47–49) are due at least in part to reduced MII·G_t coupling efficiency and slower rate of MII·G_t formation

when DHA phospholipid acyl chains are replaced by DPA. Biochemical analysis shows that the rates of G_t activation and PDE catalytic subunit activation are approximately equal (50). Assuming that the rates of G_t binding and G_t activation are similar, this means that a reduction in the rate of MII·G_t complex formation by 10% will delay the rod cell photoresponse by 5%, as calculated according to the model of Leskov *et al.* (50). The results presented here indicate that the effects of membrane composition on the rate and efficiency of receptor-G protein coupling, *via* lateral diffusion, and changes in the rate of MII formation would be sufficient to account for the delays in photoreceptor activity observed in dietary n-3 deficiency (14,47,48). Because of the similar signaling motif in other G protein–coupled signaling systems, the findings presented here should be generally applicable to other members in the G protein–coupled family, providing a molecular mechanism for the observed loss in cognitive skills (11), and odor (16) and spatial discrimination (17) observed in n-3 fatty acid deficiency.

REFERENCES

1. Simons, K., and Ehehalt, R. (2002) Cholesterol, Lipid Rafts, and Disease, *J. Clin. Investig.* 110, 597–603.
2. Ntambi, J.M., and Bene, H. (2001) Polyunsaturated Fatty Acid Regulation of Gene Expression, *J. Mol. Neurosci.* 16, 273–278.
3. Neuringer, M. (2000) Infant Vision and Retinal Function in Studies of Dietary Long-Chain Polyunsaturated Fatty Acids: Methods, Results, and Implications, *Am. J. Clin. Nutr.* 71 (1. Suppl.), 256S–267S.
4. Carlson, S.E. (2001) Docosahexaenoic Acid and Arachidonic Acid in Infant Development, *Semin. Neonatol.* 6, 437–449.
5. Koletzko, B., Agostoni, C., Carlson, S.E., Clandinin, T., Hornstra, G., Neuringer, M., Uauy, R., Yamashiro, Y., and Willatts, P. (2001) Long Chain Polyunsaturated Fatty Acids (LC-PUFA) and Perinatal Development, *Acta Paediatr.* 90, 460–464.
6. O'Brien, D.F., Costa, L.F., and Ott, R.A. (1977) Photochemical Functionality of Rhodopsin-Phospholipid Recombinant Membranes, *Biochemistry* 16, 1295–1303.
7. Wiedmann, T.S., Pates, R.D., Beach, J.M., Salmon, A., and Brown, M.F. (1988) Lipid-Protein Interactions Mediate the Photochemical Function of Rhodopsin, *Biochemistry* 27, 6469–6474.
8. Brown, M.F. (1994) Modulation of Rhodopsin Function by Properties of the Membrane Bilayer, *Chem. Phys. Lipids* 73, 159–180.
9. Bourne, H.R. (1997) How Receptors Talk to Trimeric G Proteins, *Curr. Opin. Cell Biol.* 9, 134–142.
10. Stinson, A.M., Wiegand, R.D., and Anderson, R.E. (1991) Fatty Acid and Molecular Species Compositions of Phospholipids and Diacylglycerols from Rat Retinal Membranes, *Exp. Eye Res.* 52, 218.
11. Salem, N., Jr., Hullin, F., Yoffe, A.M., Karanian, J.W., and Kim, H.Y. (1989) Fatty Acid and Phospholipid Species Composition of Rat Tissues After a Fish Oil Diet, *Adv. Prostaglandin Thromboxane Leukotriene Res.* 19, 618–622.
12. Galli, C., Trzeciak, H.I., and Paoletti, R. (1972) Effects of Essential Fatty Acid Deficiency on Myelin and Various Subcellular Structures in Rat Brain, *J. Neurochem.* 19, 1863–1867.
13. Benolken, R.M., Anderson, R.E., and Wheeler, T.G. (1973) Membrane Fatty Acids Associated with Electrical Response in Visual Excitation, *Science* 182, 1253–1254.
14. Birch, D.G., Birch, E.E., Hoffman, D.R., and Uauy, R.D. (1992) Retinal Development in Very Low Birth Weight Infants Fed

- Diets Differing in Omega-3 Fatty Acids, *Investig. Ophthalmol. Vis. Sci.* 33, 2365–2376.
15. Bourre, J.M., Francois, M., Youyou, A., Dumont, O., Picotti, M.J., Pascal, G.A., and Durand, G. (1989) The Effects of Dietary α -Linolenic Acid on the Composition of Nerve Membranes, Enzymatic Activity, a Multitude of Electrophysiological Parameters, Resistance to Poisons and Performance of Learning Tasks, *J. Nutr.* 119, 1880–1892.
 16. Greiner, R.S., Moriguchi, T., Hutton, A., Slotnick, B.M., and Salem, N., Jr. (1999) Rats with Low Levels of Brain Docosahexaenoic Acid Show Impaired Performance in Olfactory-Based and Spatial Learning Tasks, *Lipids* 34 (Suppl.), S239–S243.
 17. Moriguchi, T., Greiner, R.S., and Salem, N., Jr. (2000) Behavioral Deficits Associated with Dietary Induction of Decreased Brain Docosahexaenoic Acid Concentration, *J. Neurochem.* 75, 2563–2573.
 18. Matsuda, T., Takao, T., Shimonishi, Y., Murata, M., Asano, T., Yoshizawa, T., and Fukada, Y. (1994) Characterization of Interactions Between Transducin α/β γ -Subunits and Lipid Membranes, *J. Biol. Chem.* 269, 30358–30363.
 19. Kisselev, O.G., Ermolaeva, M.V., and Gautam, N. (1994) A Farnesylated Domain in the G Protein γ Subunit Is a Specific Determinant of Receptor Coupling, *J. Biol. Chem.* 269, 21399–21402.
 20. Seitz, H.R., Heck, M., Hofmann, K.P., Alt, T., Pellaud, J., and Seelig, A. (1999) Molecular Determinants of the Reversible Membrane Anchorage of the G-Protein Transducin, *Biochemistry* 38, 7950–7960.
 21. Ernst, O.P., Meyer, C.K., Marin, E.P., Henklein, P., Fu, W.Y., Sakmar, T.P., and Hofmann, K.P. (2000) Mutation of the Fourth Cytoplasmic Loop of Rhodopsin Affects Binding of Transducin and Peptides Derived from the Carboxyl-Terminal Sequences of Transducin α and γ Subunits, *J. Biol. Chem.* 275, 1937–1943.
 22. Farahbakhsh, Z.T., Ridge, K.D., Khorana, H.G., and Hubbell, W.L. (1995) Mapping Light-Dependent Structural Changes in the Cytoplasmic Loop Connecting Helices C and D in Rhodopsin: A Site-Directed Spin Labeling Study, *Biochemistry* 34, 8812–8819.
 23. Litman, B.J., and Mitchell, D.C. (1996) Rhodopsin Structure and Function, in *Biomembranes 2* (Lee, A.G., ed.) pp. 1–32, JAI Press, Greenwich, CT.
 24. Miller, J.L., Fox, D.A., and Litman, B.J. (1986) Amplification of Phosphodiesterase Activation Is Greatly Reduced by Rhodopsin Phosphorylation, *Biochemistry* 25, 4983–4988.
 25. Smith, H.G., Jr., Stubbs, G.W., and Litman, B.J. (1975) The Isolation and Purification of Osmotically Intact Discs from Retinal Rod Outer Segments, *Exp. Eye Res.* 20, 211–217.
 26. Litman, B.J. (1982) Purification of Rhodopsin by Concanavalin A Affinity Chromatography, *Methods Enzymol.* 81, 150–153.
 27. Jackson, M.L., and Litman, B.J. (1985) Rhodopsin-Egg Phosphatidylcholine Reconstitution by an Octyl Glucoside Dilution Procedure, *Biochim. Biophys. Acta* 812, 369–376.
 28. Miller, J.L., Litman, B.J., and Dratz, E.A. (1987) Binding and Activation of Rod Outer Segment Phosphodiesterase and Guanosine Triphosphate Binding Protein by Disc Membranes: Influence of Reassociation Method and Divalent Cations, *Biochim. Biophys. Acta* 898, 81–89.
 29. Bartlett, G.R. (1959) Colorimetric Assay Methods for Free and Phosphorylated Glyceric Acids, *J. Biol. Chem.* 234, 469–471.
 30. Niu, S.L., Mitchell, D.C., and Litman, B.J. (2002) Manipulation of Cholesterol Levels in Rod Disk Membranes by Methyl- β -Cyclodextrin: Effects on Receptor Activation, *J. Biol. Chem.* 277, 20139–20145.
 31. Straume, M., Mitchell, D.C., Miller, J.L., and Litman, B.J. (1990) Interconversion of Metarhodopsins I and II: A Branched Photo-intermediate Decay Model, *Biochemistry* 29, 9135–9142.
 32. Mitchell, D.C., Niu, S.L., and Litman, B.J. (2001) Optimization of Receptor-G Protein Coupling by Bilayer Lipid Composition I: Kinetics of Rhodopsin-Transducin Binding, *J. Biol. Chem.* 276, 42801–42806.
 33. Yee, R., and Liebman, P. (1978) Light-Activated Phosphodiesterase of the Rod Outer Segment: Kinetics and Parameters of Activation and Deactivation, *J. Biol. Chem.* 253, 8902–8909.
 34. Mitchell, D.C. (1998) Effect of Cholesterol on Molecular Order and Dynamics in Highly Polyunsaturated Phospholipid Bilayers, *Biophys. J.* 75, 896–908.
 35. Mitchell, D.C. (1998) Molecular Order and Dynamics in Bilayers Consisting of Highly Polyunsaturated Phospholipids, *Biophys. J.* 74, 879–891.
 36. Straume, M. (1987) Equilibrium and Dynamic Structure of Large, Unilamellar, Unsaturated Acyl Chain Phosphatidylcholine Vesicles. Higher Order Analysis of 1,6-Diphenyl-1,3,5-hexatriene and 1-[4-(Trimethylammonio)phenyl]-6-phenyl-1,3,5-hexatriene Anisotropy Decay, *Biochemistry* 26, 5113–5120.
 37. Johnson, M.L., and Faunt, L.M. (1992) Parameter Estimation by Least-Squares Methods, *Methods Enzymol.* 210, 1–37.
 38. Straume, M., and Litman, B.J. (1987) Influence of Cholesterol on Equilibrium and Dynamic Bilayer Structure of Unsaturated Acyl Chain Phosphatidylcholine Vesicles as Determined from Higher Order Analysis of Fluorescence Anisotropy Decay, *Biochemistry* 26, 5121–5126.
 39. Mitchell, D.C., Straume, M., Miller, J.L., and Litman, B.J. (1990) Modulation of Metarhodopsin Formation by Cholesterol-Induced Ordering of Bilayer Lipids, *Biochemistry* 29, 9143–9149.
 40. Litman, B.J., and Mitchell, D.C. (1996) A Role for Phospholipid Polyunsaturation in Modulating Membrane Protein Function, *Lipids* 31 (Suppl.), S193–S197.
 41. Niu, S.L., Mitchell, D.C., and Litman, B.J. (2001) Optimization of Receptor-G Protein Coupling by Bilayer Lipid Composition II: Formation of Metarhodopsin II-Transducin Complex, *J. Biol. Chem.* 276, 42807–42811.
 42. Nathans, J. (1992) Rhodopsin: Structure, Function, and Genetics, *Biochemistry* 31, 4923–4931.
 43. Mitchell, D.C., and Litman, B.J. (1998) Effect of Cholesterol on Molecular Order and Dynamics in Highly Polyunsaturated Phospholipid Bilayers, *Biophys. J.* 75, 896–908.
 44. Mitchell, D.C., Straume, M., and Litman, B.J. (1992) Role of *sn*-1-Saturated, *sn*-2-Polyunsaturated Phospholipids in Control of Membrane Receptor Conformational Equilibrium: Effects of Cholesterol and Acyl Chain Unsaturation on the Metarhodopsin I in Equilibrium with Metarhodopsin II Equilibrium, *Biochemistry* 31, 662–670.
 45. Lamola, A.A., Yamane, T., and Zipp, A. (1974) Effects of Detergents and High Pressures Upon the Metarhodopsin I–Metarhodopsin II Equilibrium, *Biochemistry* 13, 738–745.
 46. Hamm, H.E. (1998) The Many Faces of G Protein Signaling, *J. Biol. Chem.* 273, 669–672.
 47. Neuringer, M., Connor, W.E., Lin, D.S., Barstad, L., and Luck, S. (1986) Biochemical and Functional Effects of Prenatal and Postnatal Omega-3 Fatty Acid Deficiency on Retina and Brain in Rhesus Monkeys, *Proc. Natl. Acad. Sci. USA* 83, 4021–4025.
 48. Jeffrey, B.G., Mitchell, D.C., Gibson, R.A., and Neuringer, M. (2002) n-3 Fatty Acid Deficiency Alters Recovery of the Rod Photoresponse in Rhesus Monkeys, *Investig. Ophthalmol. Vis. Sci.* 43, 2806–2814.
 49. Birch, D.G., Birch, E.E., Hoffman, D.R., and Uauy, R.D. (1992) Retinal Development in Very Low Birth Weight Infants Fed Diets Differing in Omega-3 Fatty Acids, *Investig. Ophthalmol. Vis. Sci.* 33, 2365–2376.
 50. Leskov, I.B., Klenchin, V.A., Handy, J.W., Whitlock, G.G., Gowardovskii, V.I., Bownds, M.D., Lamb, T.D., Pugh, E.N., and Arshavsky, V.Y. (2000) The Gain of Rod Phototransduction: Reconciliation of Biochemical and Electrophysiological Measurements, *Neuron* 27, 525–537.

[Received November 8, 2002; accepted April 14, 2003]